



Queensland University of Technology
Brisbane Australia

This is the author's version of a work that was submitted/accepted for publication in the following source:

[Pourkhesalian, A.M.](#), [Stevanovic, S.](#), [Salimi, F.](#), [Rahman, M.M.](#), Wang, H., Pham, P.H., [Bottle, S.E.](#), Masri, A.R., [Brown, R.J.](#), & [Ristovski, Z.D.](#) (2014)

Influence of fuel molecular structure on the volatility and oxidative potential of biodiesel particulate matter.

Environmental Science & Technology, 48(21), pp. 12577-12585.

This file was downloaded from: <https://eprints.qut.edu.au/85905/>

© **American Chemical Society**

Author version posted with permission of publisher (for individual non-commercial use only).

Notice: *Changes introduced as a result of publishing processes such as copy-editing and formatting may not be reflected in this document. For a definitive version of this work, please refer to the published source:*

<https://doi.org/10.1021/es503160m>

21 with shorter carbon chain lengths result in lower particle mass but produce particles that are more
22 volatile and also have higher levels of Reactive Oxygen Species (ROS). This highlights the importance of
23 taking into account metrics that are relevant from the health effects point of view when assessing
24 emissions from new fuel types.

25

26 Introduction

27 Alternative and renewable sources of fuels draw a substantial amount of attention motivated by the
28 constant movement towards more stringent regulation against diesel emissions, the rising price of
29 crude oil, and the vulnerability of fossil fuel resources. Biodiesel is currently one of the most promising
30 alternatives to fossil fuels, and depending on its chemical and physical properties, may be considered as
31 a suitable choice for blending with diesel fuel to account for increasing fuel demand ¹⁻³. Biodiesel is a
32 processed fuel which is derived from biological sources by transesterifying vegetable oils, animal fats or
33 algae ³. In terms of chemical composition, biodiesel fuels are mono-alkyl esters of fatty acids ³. Most of
34 the biodiesel fuels are composed of Fatty Acid Methyl Esters (FAMES) ³. The reasons that make
35 biodiesels a suitable and practical fuel choice are numerous. They can be derived from a number of feed
36 stocks such as rapeseed, soybean, palm, waste cooking oil, tallow, jatropha, algae etc ¹⁻³. Biodiesels are
37 renewable and degradable ^{2,4}. Lack of polycyclic aromatic hydrocarbons reduces Hydro carbons (HC)
38 and Carbon monoxide (CO) concentrations in the exhaust ⁵. In addition, the oxygen content of biodiesel
39 plays an important role in reducing black carbon (BC) formation when local oxygen concentration
40 decreases due to a diffusion combustion ⁵⁻⁷. The higher cetane number of biodiesel leads to a more
41 complete combustion ⁸ which in turn results in higher levels of NOx concentration in the exhaust gas ⁹.

42 Recently, particulate matter (PM) produced by biodiesel combustion has become a popular research
43 topic ¹⁰⁻¹⁵. This is understandable considering that emissions from diesel engines have been recently
44 declared as carcinogenic ¹⁶. It is commonly seen that biodiesel causes less PM mass concentration in the
45 exhaust gas ^{10, 17, 18}. However, some studies have reported an increase in the particle number
46 concentration ^{11, 19, 20} as well as particle number per unit of particle mass ²¹. An additional concern was
47 the observation that non-petroleum diesel fuels emit excessive amounts of volatile compounds upon
48 combustion, which potentially results in more toxic emissions^{14, 22, 23}. It is also reported that combustion

49 of biodiesel generates smaller particles that can penetrate deeper in lungs causing inflammation at the
50 sites of deposition ^{12-14, 22}.

51 The quality of combustion is a key factor that affects all the outputs of an engine. Viscosity, surface
52 tension, density, cetane number, low-temperature properties (cloud point, pour point, etc.) ^{2,8}, heating
53 value and lubricity ⁸ are amongst the physical parameters of the fuel affecting the combustion process.
54 On the other hand, chemical properties such as carbon chain length, number of double bonds and the
55 amount of oxygen borne by the fuel may also affect the aforementioned physical properties and in turn,
56 the combustion process. There have been a growing number of publications that study the correlation
57 between fuel composition and engine emission, especially diesel particulate matter (DPM) ^{9, 17, 24}. The
58 relationship between biodiesel chemical properties and resulting emissions were investigated ^{2, 5, 8, 9, 24,}
59 ²⁵, and it has been found that blends with higher oxygen content produce less PM but more volatile
60 particles and increased levels of NOx ^{5, 9, 25}; while biodiesel fuels with longer carbon chain length led to
61 more PM ^{8, 24}.

62 DPM is well known for its adverse effects on humans, animals and the environment ²⁶⁻²⁸. Recently,
63 based on the current body of knowledge, the International Agency for Research on Cancer (IARC) has
64 labeled diesel exhaust as carcinogenic within class 1 ¹⁶. While the mechanism by which DPM causes the
65 adverse health effects are not known, a great deal of the harmful effects relate to its ability to cause
66 oxidative stress ²⁹⁻³⁵. Therefore, measurement of oxidative potential (OP), expressed through ROS
67 concentration, can be used as a good estimate for its reactivity and toxicity. Based on the data provided
68 in the literature so far, it remains unclear which chemical species contribute to the measured redox
69 potential and the overall toxicity. Several studies in this area showed that ^{23, 29, 36} the organic fraction,
70 more precisely semi-volatile component of PM, correlated well with the measured OP. Stevanovic et al.
71 ²⁹ further showed that the oxygenated fraction of the semi-volatile component of DPM was most
72 responsible for the OP of DPM.

73 The primary objective of this work is to critically examine the influence of the carbon chain length and
74 saturation levels of biodiesel fuel molecules on the overall volatility (OV) and OP of DPM. All the work
75 has been undertaken by investigating particle emissions from a common-rail engine using four palm oil
76 biodiesels and different blend percentages. All tested biodiesels were FAMES with controlled fatty acid
77 composition. This enabled us to assign the influence of a particular parameter more easily. This paper is
78 an extension of a previous study³⁷ where the engine performance characteristics and emissions were
79 investigated and presented, including some preliminary findings for the ROS emission, particularly for
80 pure biodiesel. It should be noted that the results for B100 are reproduced here for comparison
81 purposes. Furthermore, the paper elaborates on these findings and new analysis in terms of physico-
82 chemical properties of the fuels and their blends.

83 **Experimental setup and methodology**

84 A schematic of the experimental setup is can be found in Figure S1 in supporting information. The test
85 bed included a diesel engine coupled to a dynamometer and the accompanying instruments for PM and
86 gas measurement. The specifications of the engine and dynamometer are shown in Supporting
87 Information, Table S1. Raw diesel exhaust was sampled from the exhaust line and passed through a
88 dilution tunnel and a Dekati ejector diluter both of which were fed with HEPA-filtered air. A TSI Dustrak
89 (model 8530) measured the mass of particles. Gas analysers, consisting of a NDIR (Non-dispersive infra-
90 red) CAI 600 series CO₂ and CO analyser and a CAI 600 series CLD (Chemiluminescence detector) NOx
91 analyser, measured CO, CO₂ and NOx concentrations before the dilution system. Also, to determine the
92 dilution ratio, a SABLE CA-10 CO₂ analyser was used to measure CO₂ concentrations after each dilution
93 step. Real-time measurements of black carbon concentrations were performed by an Aethalometer
94 (AE33, 7-Wavelength). A Scanning Mobility Particle Sizer (SMPS TSI 3080, with a 3022 CPC) measured
95 the size distribution of diesel exhaust. A Volatility Tandem Differential Mobility Analyser (VTDMA)
96 consisting of an electrostatic classifier, a thermo-denuder and an SMPS (in-house designed column with

97 a 3010 CPC) measured the volatile content of particles. The VTDMA gave the change in particulate
98 diameter for six pre-selected sizes: 30, 60, 90, 120, 150, 200 and 220 nm after they passed through the
99 thermo-denuder with the temperature set at 300 °C. The flow rate through the thermo-denuder was
100 kept constant at 1 lpm, which lead to a residence time of around 2 seconds. As the concentration of
101 particles entering the thermo-denuder is rather small, there was no need to equip the thermo-denuder
102 with a charcoal section. Absorption of the evaporated semivolatiles on the walls of the thermo-denuder
103 was sufficient to reduce the vapour pressure and prevent them recondensing on to the existing
104 nonvolatile particles ³⁸.

105 The volumetric volatile fraction (*VVF*) for each size was calculated from the difference in diameter of
106 particles before and after the thermo-denuder³⁹.

107 This study approximates the fractal-like diesel aerosols by spherical particles with the corresponding
108 electrical mobility diameter. Although the mentioned assumption is not accurate for larger
109 agglomerates of diesel particles, it would not distract the results as this study aims at comparing various
110 fuels and not at quantification of the amount of volatile material emitted by combustion of biodiesel.

111 The total amount of volatile matter is calculated for every sampling point and the parameter used for its
112 quantification is the Overall Volatility (*OV*). This was previously introduced in the literature by
113 Giechaskiel ⁴⁰, where it was used for the calculation of the non-volatile fraction of PM. More details of
114 the concept and the procedure used for calculation of *OV* can be found in the supplement material.

115 The BPEA molecular probe (bis(phenylethynyl) anthracene-nitroxide) was applied in-situ to assess the
116 OP of different fuel stocks. Samples were collected by bubbling aerosol through an impinger which
117 contains 20 mL of 4 µM BPEA solution (using an AR grade dimethylsulphoxide as a solvent). More details
118 on the ROS sampling methodology, theory behind its application and proof of concept in the case of
119 various combustion sources can be found in Miljevic et al. and Stevanovic et al. ⁴¹⁻⁴⁵.

120 **Fuel Selection**

121 The present study investigates four biodiesels of controlled composition, differing in levels of
122 unsaturation, carbon chain length and oxygen content. Commercial petro-diesel was used for blending.
123 Some of the fuel properties were measured experimentally in a previous study ⁴⁶, and others were
124 estimated based on the chemical composition of methyl-esters which are shown in Supporting
125 Information, Table S2. We labeled the tested FAMES as C810, C1214, C1618 and C1875, based on the
126 number of carbon atoms in the most abundant fatty acid in that particular biodiesel stock. The Iodine
127 values of C810 and C1214 are very small, implying that they are almost fully saturated; but the large
128 difference in saponification values shows that the carbon chain length of their molecules is quite
129 different and, so is the oxygen content. The Iodine value is used in the literature as the indication of the
130 unsaturation while Saponification value presents a measure of the average molecular weight or chain
131 length ⁴⁶. Conversely, C1618 and C1875 have different iodine numbers but pretty close saponification
132 values; which indicates that the carbon chain length of their molecules is close but with different levels
133 of unsaturation. We chose these controlled fuels to be able to differentiate between the effect of
134 unsaturation and carbon chain length.

135 The engine operated on blends of 100%, 50%, 20% and 0% of biodiesel and petro-diesel namely B100,
136 B50 and B20 and B0, respectively. We conducted tests at idle, quarter (1500 and 2000 rpm) and full load
137 (1500 rpm).

138 **Results and discussion**

139 Volatility measurements

140 To estimate the thermo-denuder temperature at which the volatile content of DPM is removed,
141 measurements of the temperature dependent volatility were conducted for 30 and 150 nm particles
142 using B0 at idle (Figure S2 in the Supporting Information). The temperature was ramped from room to

143 280°C in steps of 20°C. By 180°C the 30nm particles were almost completely evaporated and the larger
144 150nm particles reached a stable size. Therefore we can be confident that at the set temperature of
145 300°C all of the volatile material has been evaporated from the diesel particles and there will be no
146 effect of the size and residence time of particles ⁴⁷.

147 The VVF, calculated using Eq.1, for all the measured particle sizes and all the fuels and blends is shown
148 in Figure S3 in the Supporting Information. Out of the 4 loads studied, the highest volatility was
149 observed for particles produced during idling. This was valid for all the measured blends and fuels. In
150 addition to the idling conditions, higher volatility was only observed at full load, while particles
151 produced at quarter load and at both speeds did not show significant volatility. For almost all of the
152 fuels and blends tested and for most of the loads, higher volatility was observed for smaller particles.
153 This is the most obvious for idling conditions where 30nm particles were mainly volatile with a VVF of
154 over 75%. Similar dependence on the volatility as a function of particle size has been observed
155 previously ^{48, 49}.

156 To get a better insight into the influence of the fuel type and blend on the VVF, from the data presented
157 in Figure S3, we calculated the OV for each of the 3 fuel blends (B20, B50 and B100) and for all 4 tested
158 modes being presented in Figure 1. Unfortunately the volatility for C1214 at B100 was not measured.

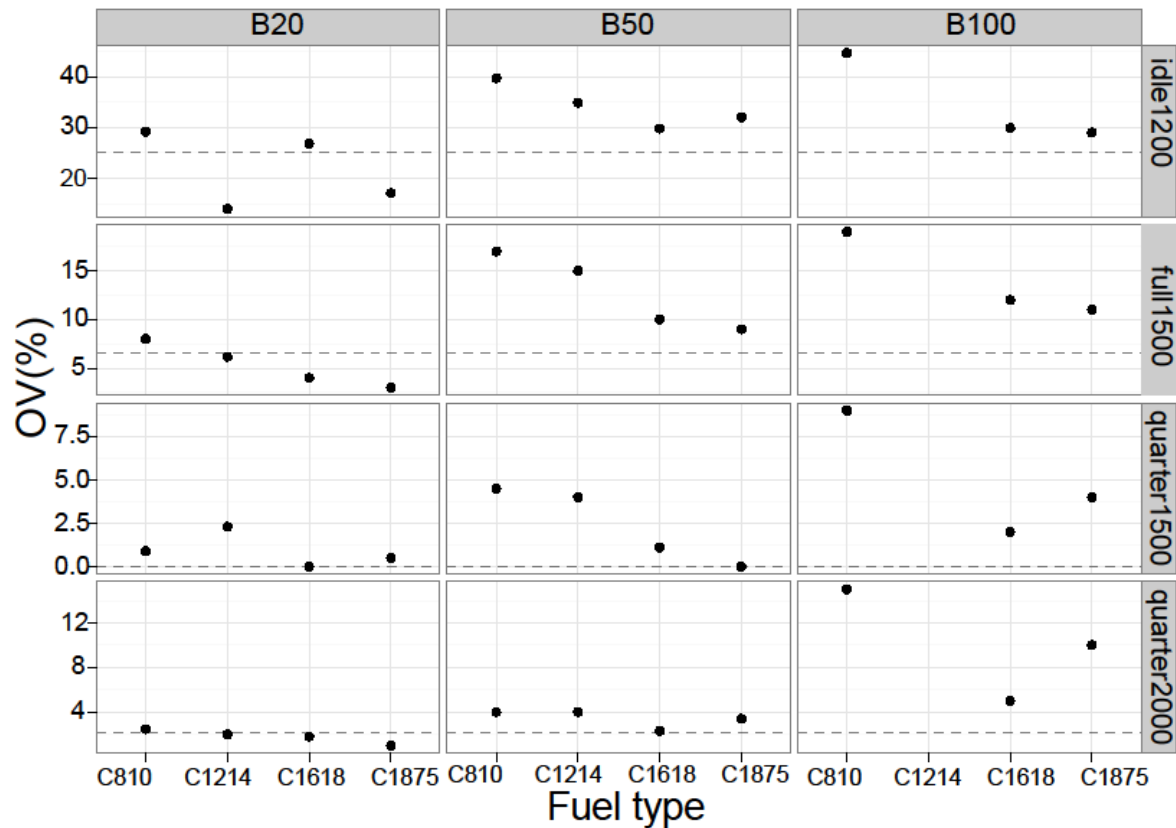


Figure 1, OV for all blends and modes tested. Rows present data measured at the same load, while columns data are measured at the same blend percentage. Different fuels are sorted along the x-axis according to their carbon chain length going from the shortest to the longest.

159 What is obvious from all of the graphs is that for all of the higher blends (B50 and B100) the measured
 160 volatility is larger than that of B0. Furthermore an increase in the volatility with the increase of the
 161 biodiesel blend percentage for the same fuel type can also be observed. While previously²³ have
 162 observed an increase in the volatility with increase in the blend percentage, the results did not show a
 163 stock dependency. In these measurements we do see a dependence on the feedstock, with the fuel with
 164 the shortest carbon chain length (C810) producing the most volatile particles for all the tests except one,
 165 B20 at quarter load and 2000 rpm. Although C810 did not produce particles with the largest OV the
 166 observed values were all within the measurement error. Also, in the case of the higher blend
 167 percentages B50 and B100, a decrease in the OV is followed by an increase in the carbon chain length.
 168 This refers to all the loads tested but is most significant at idle and full load where a larger OV was

169 measured. This is in contrast with a previous observation⁵⁰ where an increase in the volatile organic
170 fraction (VOF) was observed for an increase in the carbon chain length. It is worth mentioning that Pinzi
171 et al.⁵⁰ have used a mechanical direct-injection engines, as compared to the common rail engine used in
172 our case, for which the fuel physical properties have a significant influence on the spray pattern and
173 therefore emissions.

174 Some previous measurements conducted for petro diesel point out that the volatile part of DPM is
175 mainly due to the lubricating oil⁵¹⁻⁵³, and some recent measurements in the vicinity of busy roads also
176 show that the main contributor to the primary organic aerosol (POA) is lubricating oil from both gasoline
177 and diesel powered vehicles⁵⁴. If that was the case, in our observations, the increase in the OV could be
178 interpreted due to a decrease in the total non-volatile mass (volume) as the lubricating oil contribution
179 would be the same for all of the different fuels and blends tested.

180 On the other side, measurements on biodiesel fuels show a large fraction of fuel derived organics
181 contributing to the volatile part of DPM⁵⁵. This contribution can be as large as 90% for B50 blends⁵⁶.

182 BC Emissions

183 The change in the OV could be either due to the change in the emission of primary organic aerosol
184 (POA) or could be due to the change in the emission of the non-volatile soot component of DPM with
185 the change of the carbon chain length. A good measure of the nonvolatile mass emitted from a diesel
186 engine is the BC concentration. Figure 2 shows the BC emission factor (EF) for each of the 3 fuel blends
187 (B20, B50 and B100) and for all 4 tested modes.

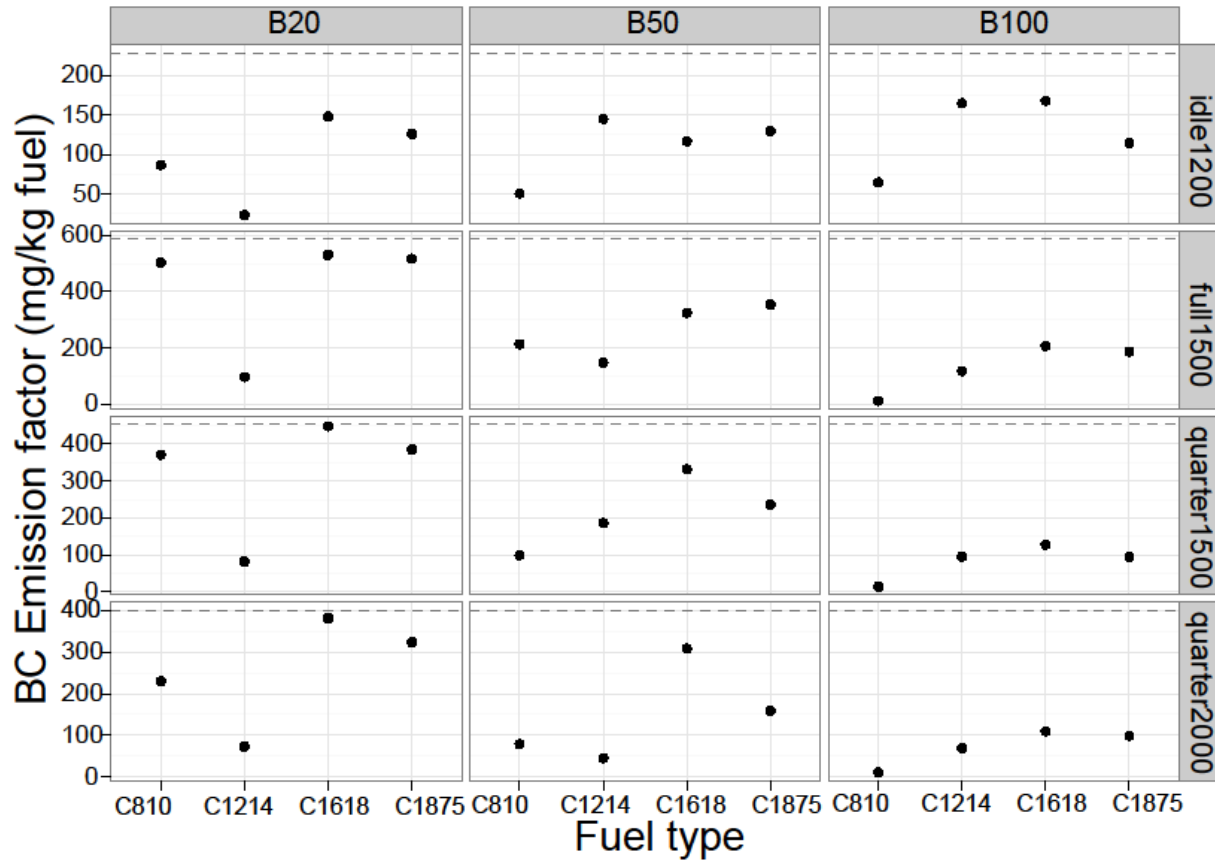


Figure 2, BC Emission factors for all blends and modes tested. The emission factor for B0 at each mode is shown as a dashed line. Rows present data measured at the same load, while columns data are measured at the same blend percentage. Different fuels are sorted along the x-axis according to their carbon chain length going from the shortest (C810) to the longest one (C1875).

188 We can see that all blends and all fuels reduce the BC emissions as compared to B0. Higher blend
 189 percentages of biodiesel (B50 and B100) show a clearer trend where the fuel with the shortest carbon
 190 chain length has the smallest BC emissions. An increase in BC emission is observed with the increase in
 191 carbon chain length up to C1618, afterwards a decrease is observed for C1875. While there is not a big
 192 difference in the carbon chain length of the FAMES that make C1618 and C1875, as both fuels contain
 193 large fraction of oleic acid of 53 and 63.5% respectively, the later fuel contains additional 28.1% of
 194 FAMES that are fully saturated (linoleic and linolenic acids). A similar increase in soot emission with the

195 increase in carbon chain length and a decrease with the level of saturation was also observed by Pinzi et
196 al.⁵⁰, although the later was not as obvious.

197 ROS measurements

198 OP measurement, expressed through ROS concentration of PM can be used as a good estimate for its
199 reactivity and toxicity. An in-house developed profluorescent molecular probe BPEAnit was applied in an
200 entirely novel, rapid and non-cell based way to assess particulate OP. Based on the data provided in the
201 literature so far⁴⁵, there are some uncertainties related to the nature of chemical species responsible for the
202 measured redox potential and overall toxicity. However, the majority of research in this field reported that
203 organic fraction, more precisely semi-volatile organic content, is in a good correlation with ROS concentration
204 ^{23, 36, 57}.

205 Figure 3 illustrates the OP of particles for the same loads and blends as for the volatility measurements
206 that were shown in Figure 1 (note logarithmic scale is used here). In idle mode, the ROS concentration is
207 much higher than in the other cases. This may be a result of the additional combustion of lubricating oil,
208 which would subsequently increase the overall organic content. Results do not show blend dependency
209 in this mode, although it is clearly visible that combustion of C810 fuel generates the largest amount of
210 ROS for all 3 blends and combustion of the fuel with the longest carbon chain length C1875 smallest
211 amount of ROS. This could be a consequence of the way the OP is presented as the concentration of ROS
212 per mass of emitted particles. As the fuels with the highest oxygen content have the lowest mass
213 emission even for the same (or similar) ROS concentration they will exhibit the highest OP when
214 calculated per unit mass of PM.

215

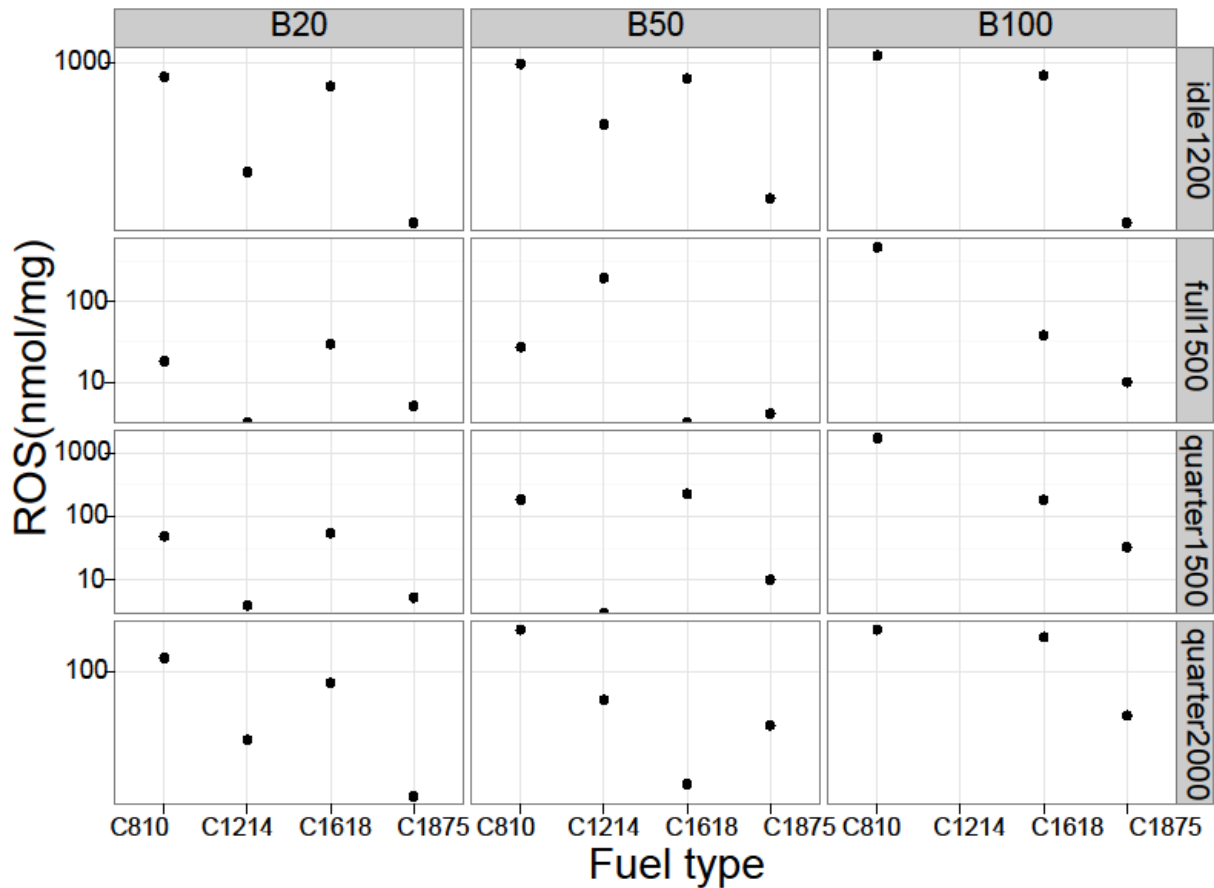


Figure 3, OP of PM for all four fuels, for all the blends and loads

216 For the other 3 loads and for most of the blends C810 produced higher ROS emissions. This is most
 217 apparent for B100, but it can also be observed even in 20 percent blends. While there is an increase in
 218 ROS emissions for 50 and 100 percent blends for all the tested fuels, C810 shows the largest increase
 219 of almost two orders of magnitude. This is a reasonable result as the C810 fuel molecules are of the
 220 shortest chain, fully saturated and with the largest oxygen content. These three parameters have
 221 synergetic effect in terms of prediction of resulting OP as have been seen previously as well ³⁷.

222 Another important parameter that will influence resulting OP is the load on the engine. Generally,
 223 engine operating conditions significantly affect physicochemical properties of emitted PM and their
 224 subsequent toxicity that were demonstrated to change with varying engine loads and speeds. Also, OP

225 tends to decrease with increasing engine load. This result can be explained by a more complete
226 combustion that results from higher temperatures and lower air to fuel ratio at higher loads. In
227 addition, at full load, the amount of lubricating oil that is available for combustion is minimal.

228 The role of oxygen content

229 As seen previously⁵⁸, out of all the fuel physical and chemical properties, oxygen content has the most
230 significant influence on particle mass and number emissions. To further investigate the influence of the
231 fuel oxygen content on particle volatility and ROS concentration, we have presented the dependence
232 of the BC emission (Figure 4), ROS emissions (Figure 5a) and OV (Figure 5b) as a function of fuel oxygen
233 content. This is done for each of the four modes tested. Oxygen content is calculated for all the fuels
234 and blends assuming that oxygen content of base-line diesel fuel is considered to be zero. As all the
235 fuels are methyl esters with varying carbon chain lengths, oxygen percentage increases with the
236 decreasing carbon chain length in respective molecules. Consequently, C810 is the fuel with the
237 highest oxygen content, followed by C1214, C1618 and finally C1875, as the fuel with the longest
238 carbon chain length as well as the most unsaturated fuel.

239 The relationships between the variables were analyzed using the linear regression or generalized linear
240 model with a log link function. The model assumptions were validated using the residuals versus fit
241 values and QQ plots. The resulting fit functions, and their 95% confidence intervals, indicate the
242 relationship between the variables. Modeling and visualizations were performed using the ggplot2
243 package in R⁵⁹.

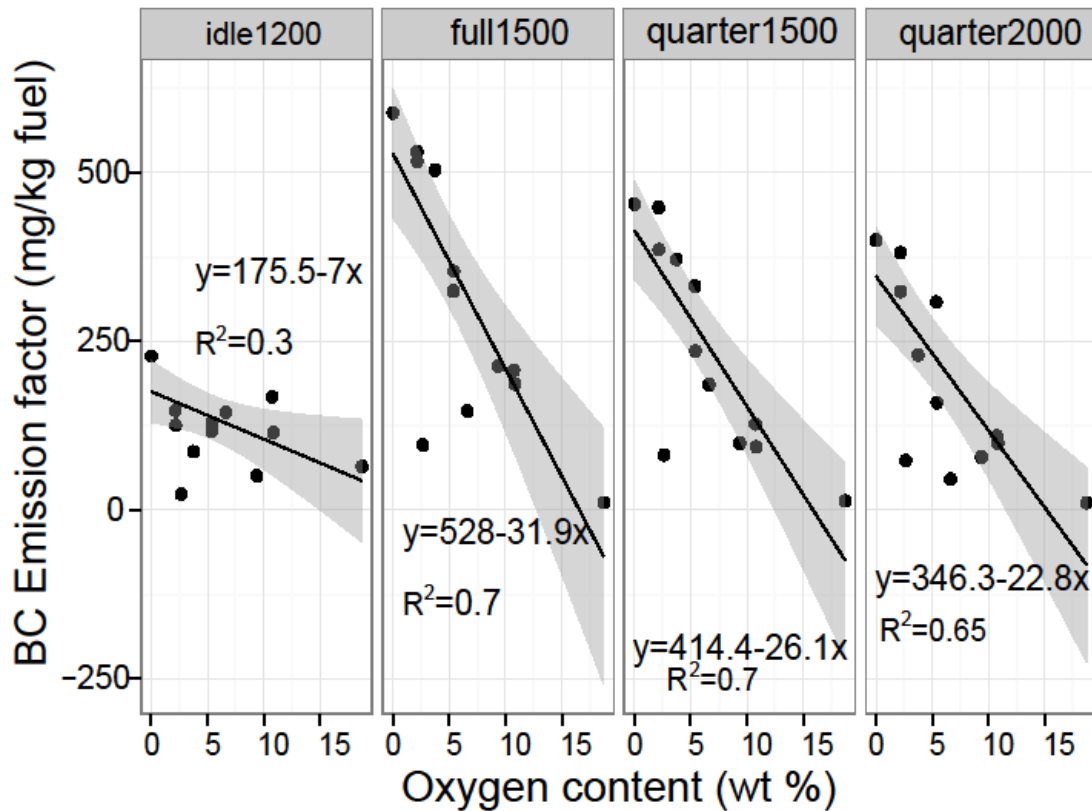


Figure 4, dependence of the BC emissions factor on fuel oxygen content for the four modes tested.

244

245 Figure 4 illustrates the decrease in the emitted BC mass with the increase of oxygen content in the
 246 fuels. The effect of oxygen content on BC formation and emissions was explained in the work of ⁶⁰Gill
 247 et al. ⁶⁰. It was suggested that oxygen present in the fuel molecule could promote the diffusion phase
 248 combustion, where soot is mainly produced, even though the diffusion phase is extended. Increased
 249 diffusion phase temperature will promote soot oxidation. Therefore the increase in oxygen content
 250 will result in a decrease in the soot or BC emissions. It is important to note that there was a linear
 251 relationship between the oxygen content and BC. Apart from idle, all other three modes showed very

252 similar trends; so on the average, BC is reduced by 270 (mg/kg fuel) per every 10 percent of increase in
 253 oxygen content in the fuel.

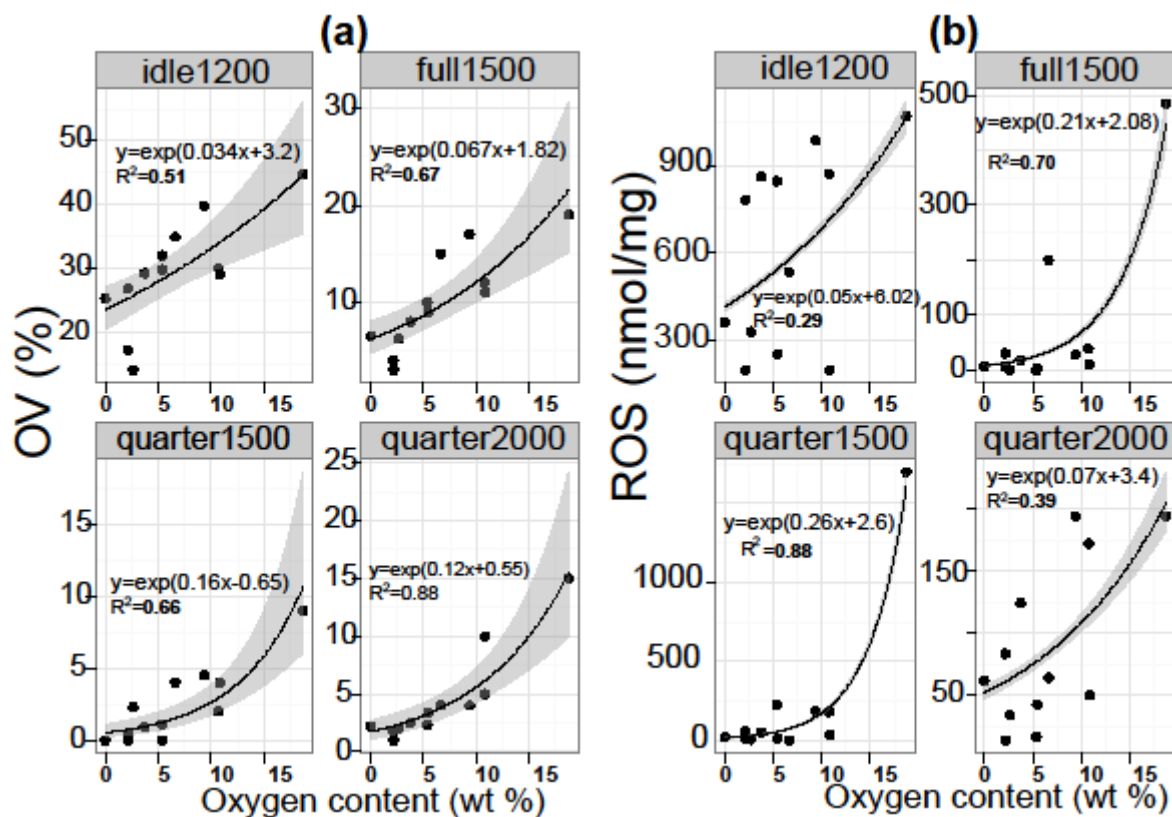


Figure 5, dependence of the a) Overall volatile content and b) ROS concentration on fuel oxygen content for the four modes tested. R² shown in the graphs are McFadden's pseudo R².

254 As can be seen from Figure 5 b) increasing the oxygen content leads to an increase in the ROS concentration,
 255 and therefore the OP of particles, for all of the modes tested. There is also an increase in the overall volatile
 256 content, or OV, as shown on Figure 5 a). It is interesting to observe that both the OP and OV do not seem to
 257 have a linear dependence on the oxygen content, as with BC, but exhibit a more complex behavior with an
 258 exponential dependency. The data also shows much more scattering for OP than the BC data and is strongly
 259 biased for the two 1500rpm modes (full and quarter) with the measurement of B100 C810 that had the
 260 highest oxygen content. Although not explicitly discussing the change in the volatile content with oxygen
 261 content, Pinzi et al.⁵⁰ saw an increase in the volatile content with an increase in the carbon chain length of the

262 fuel. As fuels with longer carbon chain length have lower oxygen content they essentially observe an opposite
263 effect. As mentioned previously, their trend could be due to the mechanical direct injection diesel engine that
264 they have used whose emissions are more sensitive to the physical properties of the fuels as compared to a
265 high-pressure common rail engine used in our case. In any case, as most of the new engines used today are
266 common rail our test seems to be more relevant. The increase in the OV can be due to either the decrease in
267 the available non-volatile soot onto which the volatiles condense or an actual increase in the amount of
268 volatile material. If the trend displayed in Fig 7 a) was linear then one of the above effects would have been
269 dominant. As the trend displayed on Fig 7 b) is non linear, in fact exponential, then one can assume that there
270 is a combination of both effects: reduction in the mass of soot and increase in the fuel derived volatile
271 (organic) material.

272 Similarly there are two processes that could lead to the increase in the OP. The first is the increase in the
273 amount of ROS that is carried by the particles that could also be seen as the increase in the OV. The second is
274 the decrease in the total mass of DPM as the OP is calculated per unit mass of particles. If the increase in the
275 OP were due only to the decrease in the total mass then the dependence on oxygen content would be a
276 reciprocal function and not an exponential. It is clear that the oxygen content plays a major role in the OP of
277 DPM and most likely this is a combination of the decrease of the total DPM and an increase of the volatile
278 organic fraction but also could be due to a change in the chemical composition of the organic fraction.

279 Figure 6 shows the dependence of the OP expressed through the ROS concentration as a function of the OV
280 for all of the 4 modes tested. If the chemical composition of the volatile organic material that contributes to
281 the OV was similar for the same mode than one would expect a linear dependence between the ROS
282 concentration and OV. While this has been observed for the same wood combustion conditions ⁴¹ and in some
283 cases even for the organic carbon in diesel exhaust ³⁶ in general, various fuels and loads produce a VVF with
284 significantly different OP ²⁹.

285 As can be seen from Figure 6, it seems that idle mode and quarter2000 mode can also be modeled with linear
286 fit. So, linear fit was also applied to those panels (i.e. idle1200 and quarter2000) to further explore the nature
287 of this correlation. Calculated R^2 values for linear fit were 0.45 and 0.27 for idle1200 and quarter2000
288 respectively. This indicates the existence of an unspecific pattern (neither exponential nor linear). The
289 explanation for this may be that for idle 1200 most of the volatile species contribute to the measured OP.
290 However these compounds are not equally reactive but still very volatile. In the case of quarter load at 2000
291 rpm, as the consequence of an incomplete combustion, a number of unburnt hydrocarbons are expected to
292 be present in the exhaust. These hydrocarbons will contribute to the OV values and do not necessarily need to
293 carry measurable oxidative potential. This phenomenon would lead to an unspecific pattern (neither
294 exponential nor linear).

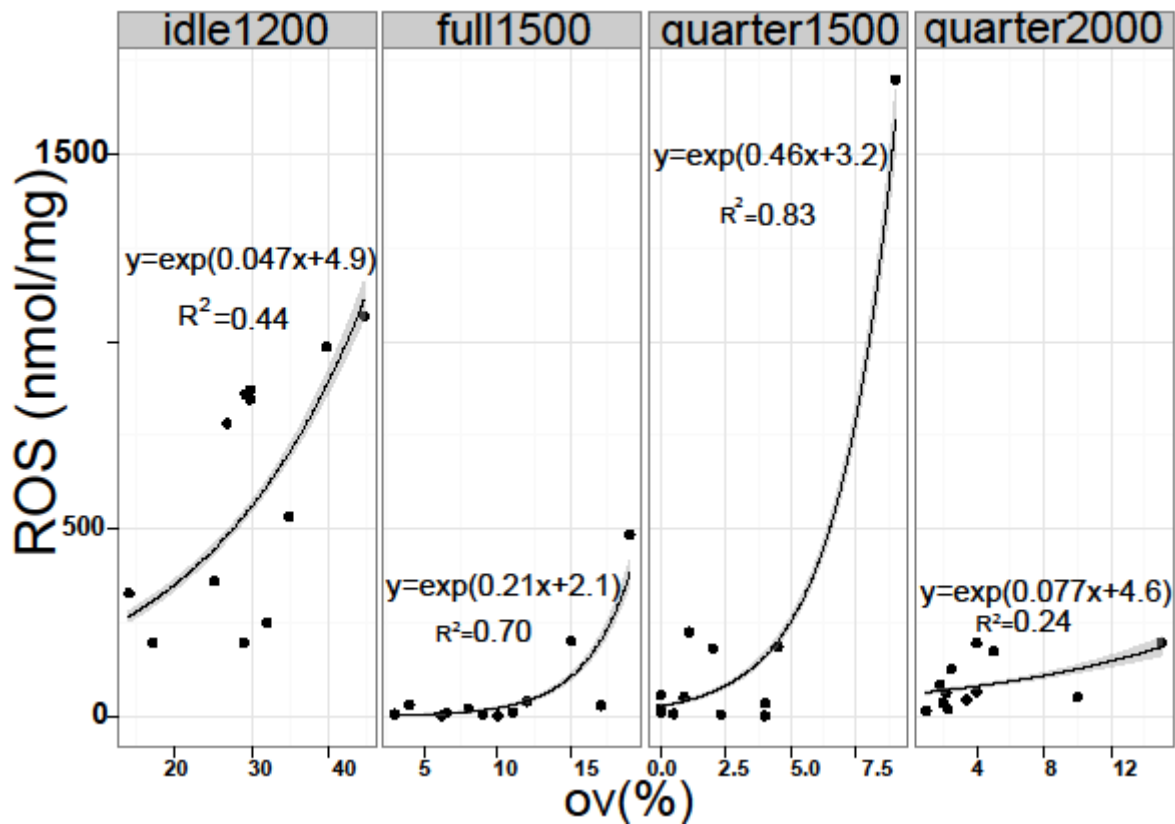


Figure 6 dependence of the ROS concentration on the overall volatile content (OV) for the 4 modes tested. R^2 shown in the graphs are McFadden's pseudo R^2 .

295 The conclusion that follows the investigation of the fuel type on the OV and related OP is that generally, the
 296 OP is ultimately coupled to the structure of fuel molecules, especially its oxygen content, chain length and
 297 level of unsaturation. It also highlights the fact that this relationship is dependent on the chemical
 298 composition of volatile matter. Even though complete combustion can yield volatile paraffins, their OP is very
 299 low compared to oxygenated organic aerosols.

300 It appears that chemical composition of volatile matter, which contributes to high levels of ROS, is different in
 301 partial and full load and therefore a more detailed chemical analysis of the organic content of DPM is required
 302 to shed more light on the toxicity of DPM. The findings of this research show that the more saturated fuels
 303 caused more potentially toxic substances in the exhaust; and even though the more oxygenated fuels
 304 decreased PM, they also led to higher levels of ROS in the particles. It was established that the majority of the
 305 redox activity is due to the amount of organics in the PM. This highlights the fact that "less PM" does not

306 necessarily mean less harmful effect for the environment or less toxicity for humans and that new metrics
307 (taking into account the potentially toxic parts of DPM) should be considered.

308 **Acknowledgments**

309 The authors would like to acknowledge the support from the Australian Research Council under Grants
310 LP110200158, DP1097125, DP130104904, DP110105535 and DP120100126. Laboratory assistance from Mr
311 Noel Hartnett and Mr Scott Abbett were also appreciated.

312 **Supporting Information Available**

313 Engine specifications, fuels properties, schematic of experimental setup along with a VTDMA scan and
314 explanation of VVF and OV concept and estimation procedure can be found in Supporting Information. This
315 information is available free of charge via the Internet at <http://pubs.acs.org/>

316 **References:**

- 317 1. Ma, F.; Hanna, M. A., Biodiesel production: a review. *Bioresource Technology* **1999**, *70*, (1), 1-15.
- 318 2. Li, Y.; Tian, G.; Xu, H., Application of Biodiesel in Automotive Diesel Engines. **2013**.
- 319 3. Demirbas, A., *Biodiesel: a realistic fuel alternative for diesel engines*. Springer: 2008.
- 320 4. Zhang, X.; Peterson, C.; Reece, D.; Haws, R.; Moller, G., Biodegradability of biodiesel in the
321 aquatic environment. *Transactions of the ASAE* **1998**, *41*, (5), 1423-1430.
- 322 5. Wang, J.; Wu, F.; Xiao, J.; Shuai, S., Oxygenated blend design and its effects on reducing diesel
323 particulate emissions. *Fuel* **2009**, *88*, (10), 2037-2045.
- 324 6. Graboski, M. S.; McCormick, R. L., Combustion of fat and vegetable oil derived fuels in diesel
325 engines. *Progress in Energy and Combustion Science* **1998**, *24*, (2), 125-164.
- 326 7. Song, J.; Lee, K., Fuel Property Impacts on Diesel Particulate Morphology, Nanostructures, and
327 NOx Emissions. *SAE Technical Paper* **2007**, 01-0129.
- 328 8. Knothe, G., Dependence of biodiesel fuel properties on the structure of fatty acid alkyl esters.
329 *Fuel processing technology* **2005**, *86*, (10), 1059-1070.
- 330 9. Knothe, G.; Sharp, C. A.; Ryan III, T. W., Exhaust emissions of biodiesel, petrodiesel, neat methyl
331 esters, and alkanes in a new technology engine. *Energy & Fuels* **2006**, *20*, (1), 403-408.
- 332 10. Cheng, C. H.; Cheung, C. S.; Chan, T. L.; Lee, S. C.; Yao, C. D., Experimental investigation on the
333 performance, gaseous and particulate emissions of a methanol fumigated diesel engine. *Science of the*
334 *Total Environment* **2008**, *389*, (1), 115-124.
- 335 11. Cheng, C. H.; Cheung, C. S.; Chan, T. L.; Lee, S. C.; Yao, C. D.; Tsang, K. S., Comparison of
336 emissions of a direct injection diesel engine operating on biodiesel with emulsified and fumigated
337 methanol. *Fuel* **2008**, *87*, (10-11), 1870-1879.

- 338 12. Cheung, K. L.; Polidori, A.; Ntziachristos, L.; Tzamkiozis, T.; Samaras, Z.; Cassee, F. R.; Gerlofs, M.;
339 Sioutas, C., Chemical Characteristics and Oxidative Potential of Particulate Matter Emissions from
340 Gasoline, Diesel, and Biodiesel Cars. *Environmental Science & Technology* **2009**, *43*, (16), 6334-6340.
- 341 13. Surawski, N. C.; Miljevic, B.; Ayoko, G. A.; Roberts, B. A.; Elbagir, S.; Fairfull-Smith, K. E.; Bottle, S.
342 E.; Ristovski, Z. D., Physicochemical Characterization of Particulate Emissions from a Compression
343 Ignition Engine Employing Two Injection Technologies and Three Fuels. *Environmental Science &*
344 *Technology* **2011**, *45*, (13), 5498-5505.
- 345 14. Sidhu, S.; Graham, J.; Striebich, R., Semi-volatile and particulate emissions from the combustion
346 of alternative diesel fuels. *Chemosphere* **2001**, *42*, (5-7), 681-690.
- 347 15. Kumar, P.; Robins, A.; Vardoulakis, S.; Britter, R., A review of the characteristics of nanoparticles
348 in the urban atmosphere and the prospects for developing regulatory controls. *Atmospheric*
349 *Environment* **2010**, *44*, (39), 5035-5052.
- 350 16. Benbrahim-Tallaa, L.; Baan, R.; Grosse, Y.; Lauby-Secretan, B.; El Ghissassi, F.; Bouvard, V.; Guha,
351 N.; Loomis, D.; Straif, K., International agency for research on cancer monograph working group.
352 Carcinogenicity of diesel-engine and gasoline-engine exhausts and some nitroarenes. *Lancet Oncol*
353 **2012**, *13*, (7), 663-4.
- 354 17. Tinsdale, M.; Price, P.; Chen, R., The impact of biodiesel on particle number, size and mass
355 emissions from a Euro4 diesel vehicle. **2010**.
- 356 18. Kalligeros, S.; Zannikos, F.; Stournas, S.; Lois, E.; Anastopoulos, G.; Teas, C.; Sakellariopoulos, F.,
357 An investigation of using biodiesel/marine diesel blends on the performance of a stationary diesel
358 engine. *Biomass and Bioenergy* **2003**, *24*, (2), 141-149.
- 359 19. Fontaras, G.; Karavalakis, G.; Kousoulidou, M.; Tzamkiozis, T.; Ntziachristos, L.; Bakeas, E.;
360 Stournas, S.; Samaras, Z., Effects of biodiesel on passenger car fuel consumption, regulated and non-
361 regulated pollutant emissions over legislated and real-world driving cycles. *Fuel* **2009**, *88*, (9), 1608-
362 1617.
- 363 20. Lee, H.; Myung, C. L.; Park, S., Time-resolved particle emission and size distribution
364 characteristics during dynamic engine operation conditions with ethanol-blended fuels. *Fuel* **2009**, *88*,
365 (9), 1680-1686.
- 366 21. Pham, P. X.; Bodisco, T. A.; Ristovski, Z. D.; Brown, R. J.; Masri, A. R., The influence of fatty acid
367 methyl ester profiles on inter-cycle variability in a heavy duty compression ignition engine. *Fuel* **2014**,
368 *116*, (0), 140-150.
- 369 22. Liu, Y. Y.; Lin, T. C.; Wang, Y. J.; Ho, W. L., Biological toxicities of emissions from an unmodified
370 engine fueled with diesel and biodiesel blend. *Journal of Environmental Science and Health Part a-*
371 *Toxic/Hazardous Substances & Environmental Engineering* **2008**, *43*, (14), 1735-1743.
- 372 23. Surawski, N. C.; Miljevic, B.; Ayoko, G. A.; Elbagir, S.; Stevanovic, S.; Fairfull-Smith, K. E.; Bottle,
373 S. E.; Ristovski, Z. D., Physicochemical characterization of particulate emissions from a compression
374 ignition engine: the influence of biodiesel feedstock. *Environmental Science & Technology* **2011**, *45*,
375 (24), 10337-43.
- 376 24. Pinzi, S.; Rounce, P.; Herreros, J. M.; Tsolakis, A.; Pilar Dorado, M., The effect of biodiesel fatty
377 acid composition on combustion and diesel engine exhaust emissions. *Fuel* **2012**.
- 378 25. Zhu, R.; Cheung, C. S.; Huang, Z., Particulate Emission Characteristics of a Compression Ignition
379 Engine Fueled with Diesel-DMC Blends. *Aerosol Science and Technology* **2011**, *45*, (2), 137-147.
- 380 26. Kim, S.; Shen, S.; Sioutas, C.; Zhu, Y. F.; Hinds, W. C., Size distribution and diurnal and seasonal
381 trends of ultrafine particles in source and receptor sites of the Los Angeles basin. *Journal of the Air &*
382 *Waste Management Association* **2002**, *52*, (3), 297-307.
- 383 27. McClellan, R. O., HEALTH-EFFECTS OF EXPOSURE TO DIESEL EXHAUST PARTICLES. *Annual Review*
384 *of Pharmacology and Toxicology* **1987**, *27*, 279-300.

- 385 28. Giechaskiel, B.; Alföldy, B.; Drossinos, Y., A metric for health effects studies of diesel exhaust
386 particles. *Journal of Aerosol Science* **2009**, *40*, (8), 639-651.
- 387 29. Stevanovic, S.; Miljevic, B.; Surawski, N.; Fairfull-Smith, K. E.; Bottle, S. E.; Brown, R.; Ristovski, Z.
388 D., The influence of oxygenated organic aerosols (OOA) on the oxidative potential of diesel and
389 biodiesel particulate matter. *Environmental Science & Technology* **2013**, *47*, (14), 7655-7662.
- 390 30. Ristovski, Z. D.; Miljevic, B.; Surawski, N. C.; Morawska, L.; Fong, K. M.; Goh, F.; Yang, I. A.,
391 Respiratory health effects of diesel particulate matter. *Respirology* **2012**, *17*, (2), 201-12.
- 392 31. Li, Q.; Wyatt, A.; Kamens, R. M., Oxidant generation and toxicity enhancement of aged-diesel
393 exhaust. *Atmospheric Environment* **2009**, *43*, (5), 1037-1042.
- 394 32. Shinyashiki, M.; Eiguren-Fernandez, A.; Schmitz, D. A.; Di Stefano, E.; Li, N.; Linak, W. P.; Cho, S.
395 H.; Froines, J. R.; Cho, A. K., Electrophilic and redox properties of diesel exhaust particles. *Environmental*
396 *Research* **2009**, *109*, (3), 239-244.
- 397 33. Jalava, P. I.; Tapanainen, M.; Kuusalo, K.; Markkanen, A.; Hakulinen, P.; Happonen, M. S.;
398 Pennanen, A. S.; Ihalainen, M.; Yli-Pirila, P.; Makkonen, U.; Teinila, K.; Maki-Paakkanen, J.; Salonen, R.
399 O.; Jokiniemi, J.; Hirvonen, M. R., Toxicological effects of emission particles from fossil- and biodiesel-
400 fueled diesel engine with and without DOC/POC catalytic converter. *Inhalation Toxicology* **2010**, *22*, 48-
401 58.
- 402 34. Kipen, H. M.; Gandhi, S.; Rich, D. Q.; Ohman-Strickland, P.; Laumbach, R.; Fan, Z. H.; Chen, L.;
403 Laskin, D. L.; Zhang, J. F.; Madura, K., Acute Decreases in Proteasome Pathway Activity after Inhalation
404 of Fresh Diesel Exhaust or Secondary Organic Aerosol. *Environmental Health Perspectives* **2011**, *119*, (5),
405 658-663.
- 406 35. Kooter, I. M.; van Vugt, M.; Jedynska, A. D.; Tromp, P. C.; Houtzager, M. M. G.; Verbeek, R. P.;
407 Kadijk, G.; Mulderij, M.; Krul, C. A. M., Toxicological characterization of diesel engine emissions using
408 biodiesel and a closed soot filter. *Atmospheric Environment* **2011**, *45*, (8), 1574-1580.
- 409 36. Biswas, S.; Verma, V.; Schauer, J. J.; Cassee, F. R.; Cho, A. K.; Sioutas, C., Oxidative Potential of
410 Semi-Volatile and Non Volatile Particulate Matter (PM) from Heavy-Duty Vehicles Retrofitted with
411 Emission Control Technologies. *Environmental Science & Technology* **2009**, *43*, (10), 3905-3912.
- 412 37. Pham, P.; Bodisco, T.; Stevanovic, S.; Rahman, M.; Wang, H.; Ristovski, Z.; Brown, R.; Masri, A.
413 *Engine performance characteristics for biodiesels of different degrees of saturation and carbon chain*
414 *lengths*; SAE Technical Paper: 2013.
- 415 38. Orsini, D. A.; Wiedensohler, A.; Stratmann, F.; Covert, D. S., A new volatility tandem differential
416 mobility analyzer to measure the volatile sulfuric acid aerosol fraction. *Journal of Atmospheric and*
417 *Oceanic Technology* **1999**, *16*, (6), 760-772.
- 418 39. Leskinen, A. P.; Jokiniemi, J. K.; Lehtinen, K. E. J., Characterization of aging wood chip
419 combustion aerosol in an environmental chamber. *Atmospheric Environment* **2007**, *41*, (17), 3713-3721.
- 420 40. Giechaskiel, B.; Alföldy, B.; Drossinos, Y., A metric for health effects studies of diesel exhaust
421 particles. *Journal of Aerosol Science* **2009**, *40*, (8), 639-651.
- 422 41. Miljevic, B.; Heringa, M. F.; Keller, A.; Meyer, N. K.; Good, J.; Lauber, A.; Decarlo, P. F.; Fairfull-
423 Smith, K. E.; Nussbaumer, T.; Burtscher, H.; Prevot, A. S. H.; Baltensperger, U.; Bottle, S. E.; Ristovski, Z.
424 D., Oxidative Potential of Logwood and Pellet Burning Particles Assessed by a Novel Profluorescent
425 Nitroxide Probe. *Environmental Science & Technology* **2010**, *44*, (17), 6601-6607.
- 426 42. Stevanovic, S.; Miljevic, B.; Eaglesham, G. K.; Bottle, S. E.; Ristovski, Z. D.; Fairfull-Smith, K. E.,
427 The Use of a Nitroxide Probe in DMSO to Capture Free Radicals in Particulate Pollution. *European*
428 *Journal of Organic Chemistry* **2012**, *2012*, (30), 5908-5912.
- 429 43. Stevanovic, S.; Miljevic, B.; Surawski, N. C.; Fairfull-Smith, K. E.; Bottle, S. E.; Brown, R.; Ristovski,
430 Z. D., Influence of Oxygenated Organic Aerosols (OOAs) on the Oxidative Potential of Diesel and
431 Biodiesel Particulate Matter. *Environmental Science & Technology* **2013**, *47*, (14), 7655-7662.

- 432 44. Miljevic, B.; Modini, R. L.; Bottle, S. E.; Ristovski, Z. D., On the efficiency of impingers with fritted
433 nozzle tip for collection of ultrafine particles. *Atmospheric Environment* **2009**, *43*, (6), 1372-1376.
- 434 45. Stevanovic, S.; Ristovski, Z. D.; Miljevic, B.; Fairfull-Smith, K. E.; Bottle, S. E., APPLICATION OF
435 PROFLUORESCENT NITROXIDES FOR MEASUREMENTS OF OXIDATIVE CAPACITY OF COMBUSTION
436 GENERATED PARTICLES. *Chemical Industry & Chemical Engineering Quarterly* **2012**, *18*, (4), 653-659.
- 437 46. Islam, M.; Magnusson, M.; Brown, R.; Ayoko, G.; Nabi, M.; Heimann, K., Microalgal Species
438 Selection for Biodiesel Production Based on Fuel Properties Derived from Fatty Acid Profiles. *Energies*
439 **2013**, *6*, (11), 5676-5702.
- 440 47. Riipinen, I.; Pierce, J. R.; Donahue, N. M.; Pandis, S. N., Equilibration time scales of organic
441 aerosol inside thermodenuders: Evaporation kinetics versus thermodynamics. *Atmos Environ* **2010**, *44*,
442 (5), 597-607.
- 443 48. Kwon, S. B.; Lee, K. W.; Saito, K.; Shinozaki, O., Size-Dependent Volatility of Diesel
444 Nanoparticles: Chassis Dynamometer Experiments - Environmental Science & Technology (ACS
445 Publications). ... *science & technology* **2003**.
- 446 49. Ristimäki, J.; Vaarasmahti, K.; Lappi, M.; Keskinen, J., Hydrocarbon Condensation in Heavy-Duty
447 Diesel Exhaust. *Environmental Science & Technology* **2007**, *41*, (18), 6397-6402.
- 448 50. Pinzi, S.; Rounce, P.; Herreros, J. M.; Tsolakis, A.; Pilar Dorado, M., The effect of biodiesel fatty
449 acid composition on combustion and diesel engine exhaust emissions. *Fuel* **2013**, *104*, 170-182.
- 450 51. Kittelson, D. B.; Watts, W. F.; Johnson, J. P., On-road and laboratory evaluation of combustion
451 aerosols, Part 1: Summary of diesel engine results. *J Aerosol Sci* **2006**, *37*, (8), 913-930.
- 452 52. Sakurai, H.; Park, K.; McMurry, P. H.; Zurling, D. D.; Kittelson, D. B.; Ziemann, P. J., Size-
453 dependent mixing characteristics of volatile and nonvolatile components in diesel exhaust aerosols.
454 *Environmental Science & Technology* **2003**, *37*, (24), 5487-5495.
- 455 53. Sakurai, H.; Tobias, H. J.; Park, K.; Zurling, D.; Docherty, K. S.; Kittelson, D. B.; McMurry, P. H.;
456 Ziemann, P. J., On-line measurements of diesel nanoparticle composition and volatility. *Atmos Environ*
457 **2003**, *37*, (9-10), 1199-1210.
- 458 54. Worton, D. R.; Isaacman, G.; Gentner, D. R.; Dallmann, T. R.; Chan, A. W. H.; Ruehl, C.;
459 Kirchstetter, T. W.; Wilson, K. R.; Harley, R. A.; Goldstein, A. H., Lubricating Oil Dominates Primary
460 Organic Aerosol Emissions from Motor Vehicles. *Environmental Science & Technology* **2014**, *48*, (7),
461 3698-3706.
- 462 55. Sadiqsis, I.; Koegler, J. H.; Benham, T.; Bergvall, C.; Westerholm, R., Particulate associated
463 polycyclic aromatic hydrocarbon exhaust emissions from a portable power generator fueled with three
464 different fuels—A comparison between petroleum diesel and two biodiesels. *Fuel* **2014**, *115*, 573-580.
- 465 56. Grigoratos, T.; Fontaras, G.; Kalogirou, M.; Samara, C.; Samaras, Z.; Rose, K., Effect of rapeseed
466 methylester blending on diesel passenger car emissions Part 2: Unregulated emissions and oxidation
467 activity. *Fuel* **2014**, *128*, (C), 260-267.
- 468 57. Miljevic, B.; Heringa, M. F.; Keller, A.; Meyer, N. K.; Good, J.; Lauber, A.; Decarlo, P. F.; Fairfull-
469 Smith, K. E.; Nussbaumer, T.; Burtscher, H.; Prevot, A. S.; Baltensperger, U.; Bottle, S. E.; Ristovski, Z. D.,
470 Oxidative potential of logwood and pellet burning particles assessed by a novel profluorescent nitroxide
471 probe. *Environmental Science & Technology* **2010**, *44*, (17), 6601-7.
- 472 58. Rahman, M. M.; Pourkhesalian, A. M.; Jahirul, M. I.; Stevanovic, S.; Pham, P. X.; Wang, H.; Masri,
473 A. R.; Brown, R. J.; Ristovski, Z. D., Particle emissions from biodiesels with different physical properties
474 and chemical composition. *Fuel* **2014**, *134*, (0), 201-208.
- 475 59. Wickham, H., *ggplot2: elegant graphics for data analysis*. Springer: 2009.
- 476 60. Gill, S. S.; Tsolakis, A.; Herreros, J. M.; York, A. P. E., Diesel emissions improvements through the
477 use of biodiesel or oxygenated blending components. *Fuel* **2012**, *95*, 578-586.

